# Invasive breast tumors are characterized by the presence of crystalline nanoparticles

Elena Tsolaki[1,3], William Doran[1], Luca Magnani[2], Alessandro Olivo[1], Inge K. Herrmann[3,4], Sergio Bertazzo[1]*

[1]Department of Medical Physics & Biomedical Engineering, University College London, Gower Street, London WC1E 6BT, UK.

[2]Department of Surgery and Cancer, Imperial College London, Hammersmith Hospital Campus, Du Cane Road, London W12 0NN, UK

[3]Department Materials Meet Life, Swiss Federal Laboratories for Materials Science and Technology (Empa), Lerchenfeldstrasse 5, CH-9014, St. Gallen, Switzerland.

[4]Nanoparticle Systems Engineering Laboratory, Department of Mechanical and Process Engineering, ETH Zurich, Sonneggstrasse 3, 8092 Zurich, Switzerland.

*Correspondence and requests for materials should be addressed to S.B. (email: s.bertazzo@ucl.ac.uk).

***The presence of calcification in tumours has been known for decades[1]. Indeed, calcified breast tissue is a fundamental criterion for early breast cancer diagnosis, indicative of malignancies[2], and their appearance is used to distinguish between benign and malignant in breast biopsies[3,4]. However, an in-depth characterization of the nature and origin of tumour tissue calcification remains elusive[5-8]. Here, we report the presence of nano and micron-sized spherical particles made of highly crystalline whitlockite that are exclusively found in the arterial wall of malignant invasive tumours. By applying nanoanalytical methods to healthy, benign and malignant tumour breast tissue biopsies from patients, we show that poorly crystalline apatite can be found in all breast tissue samples, whereas spherical crystalline whitlockite particles are present only in invasive cancers, mainly in areas close to the lumen of the arterial wall. Moreover, we demonstrate that the concentration of these spherical crystalline particles increases with the grade of disease, and that their size can be related to tumour type. Therefore, our results not only provide new insight into calcification***

***of tumour tissue, but also enable a precise, yet simple route of breast cancer diagnosis and staging.***

The detection of minerals in breast tissue is key to the early diagnosis of breast cancer[3,9,10]. Breast screenings are widely used to examine for the presence of calcifications, which are, in many cases, the only detectable sign of a tumour[11]. These calcifications are found in all types and grades of breast tumours[11,12-16]. A robust understanding of the physico-chemical characteristics of calcifications may shed light on the nature of the calcification of tumours, and allow a correlation between calcification and tumour type and grade.

Here, we report the distinct mineral characteristics and features of calcifications of breast tumour tissue. Initially we carried out a double-blind analysis of histological slides obtained from breast tissue biopsies of 81 patients with tumours of all grades, using density-dependent colour scanning electron microscopy (DDC-SEM)[17]. 11 tissue samples were from healthy donors, 23 samples from patients with benign tumours, and 47 samples from patients with malignant tumours, of which 8 tumours had been classed as invasive lobular, 7 as cribriform and 16 as ductal carcinomas (Supplementary information Table S1).

The electron micrographs show that calcification occurs in two forms: large deposits made of compact calcification (Fig. 1a, Supplementary Fig S1) with no specific morphology and dimensions ranging from 10 μm to 300 μm, and spherical particles (Fig. 1b, c, d, Supplementary Fig S2). Large deposits of compact calcification were found in 18% of the samples from healthy donors, in 11% of the samples from patients with benign tumours and in 62% of the samples of patients with invasive malignant tumours (Fig. 1e). Interestingly, particles (with sizes ranging from 46 nm to 2200 nm, average size of 434.0 ± 0.2 nm, Fig. 1f) are present only in invasive cribriform (Fig. 1b), invasive lobular (Fig. 1c) and invasive ductal carcinoma (Fig. 1d) samples. Moreover, compact calcification was observed in different breast tissue types, including the ducts and the stroma; by contrast, particles were only detected in arteries.

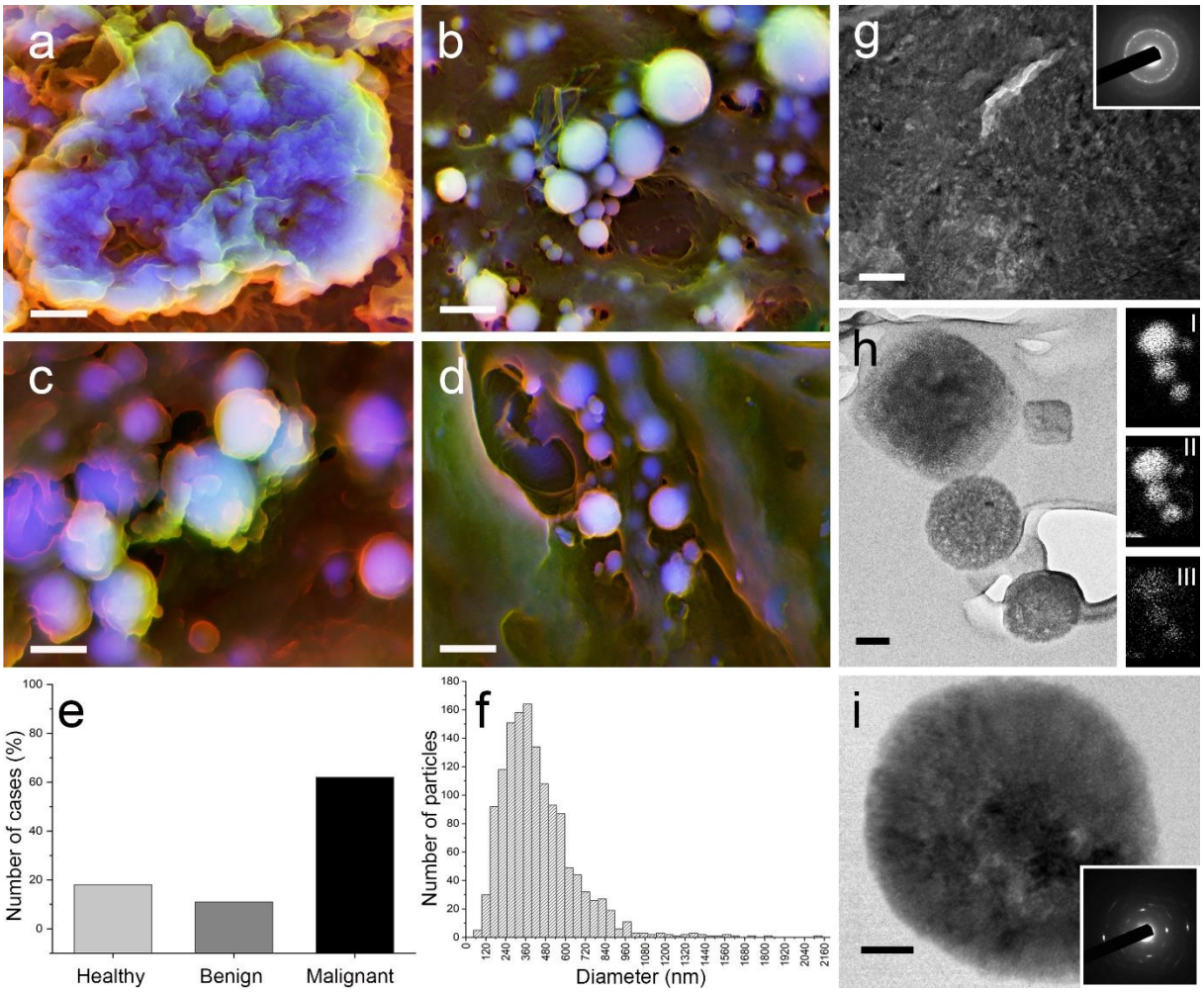


**Figure 1. Representative electron micrographs and chemical analysis of compact calcification and particles in breast tissue samples. a** DDC-SEM representative micrograph of compact calcification present in a benign sclerosing papillary case. Scale bar = 3 µm. **b** DDC-SEM representative micrograph of particles in a malignant invasive cribriform carcinoma. Scale bar = 2 µm. **c** DDC-SEM representative micrograph of particles in a malignant invasive lobular carcinoma. Scale bar = 300 nm. **d** DDC-SEM representative micrograph of particles in a malignant invasive ductal carcinoma. Scale bar = 1 µm. Blue and purple colours correspond to dense material (minerals), whereas structures that appear in green and red correspond to lower density materials (extracellular matrix and cells). **e** Histogram indicating the percentage of cases in which calcification was detected. **f** Size distribution of 1300 particles observed in malignant invasive tumours. **g** TEM micrograph of large mineral in a benign phyllodes tumour sample and corresponding SAED pattern, indicating hydroxyapatite of polycrystalline structure. The full width half maximum (FWHM) indicates a value of 5.302. Scale bar = 100 nm. **h** TEM micrograph of calcified particles in a malignant invasive lobular carcinoma sample, and elemental mapping of the same particles, showing **I** calcium (Ca), **II** phosphorus (P) and **III** magnesium (Mg). Scale bar = 100nm. **i** TEM micrograph of nanoparticles in a malignant invasive cribriform carcinoma sample, with SAED pattern indicating whitlockite diffracting as a highly crystalline single crystal. FWHM indicates a value of 1.042. Scale bar = 50 nm.

After DDC-SEM we then applied transmission electron microscopy with energy dispersive x-ray spectroscopy (TEM-EDS) and selective area electron diffraction (SAED) to calcified tissue samples sectioned by focused ion beam (FIB). Compact calcifications have no consistent internal structure (Fig. 1g), and are composed of calcium phosphate (Supplementary Fig S3 (EDS spectra)) in the form of polycrystalline hydroxyapatite (Fig. 1g insert). By contrast, the internal structure of the calcified particles consists of concentric crystals (Fig. 1h and i). The particles are composed of calcium and phosphorus, with small amounts of magnesium (Fig. 1h and Supplementary Fig S3). Their SAED diffraction pattern shows that particles diffract as a whitlockite single crystal (Fig. 1i). The presence of hydroxyapatite[9,18,19] and whitlockite[7,12,18,20] has previously been acknowledged in breast cancer calcifications; however, to the best of our knowledge, this is the first report of two distinct mineral structures and the presence of distinct calcified particles only in malignant breast tumours.

In the arteries, the majority of particles are located close to the lumen (Fig. 2a, Supplementary Fig. S4, S5). Notably, they are concentrated in the internal elastic lamina[21] (Fig. 2b), with 90% of particles within 50 µm of the lumen, and all particles within 100 µm of the lumen. There is no statistically significant association of particle size and type of invasive carcinoma (Fig. 2c). However, particle size and grade of cancer can be correlated; the size of particles in samples of grade 1 tumours was found to be slightly larger than in samples of grade 2 and grade 3 tumours (Fig. 2d). Moreover, the fact that the average radius of the particles remains relatively constant across all grades and types of malignancies would maybe suggests that the particles originate from mineralizing elements which are constantly provided to the arteries.

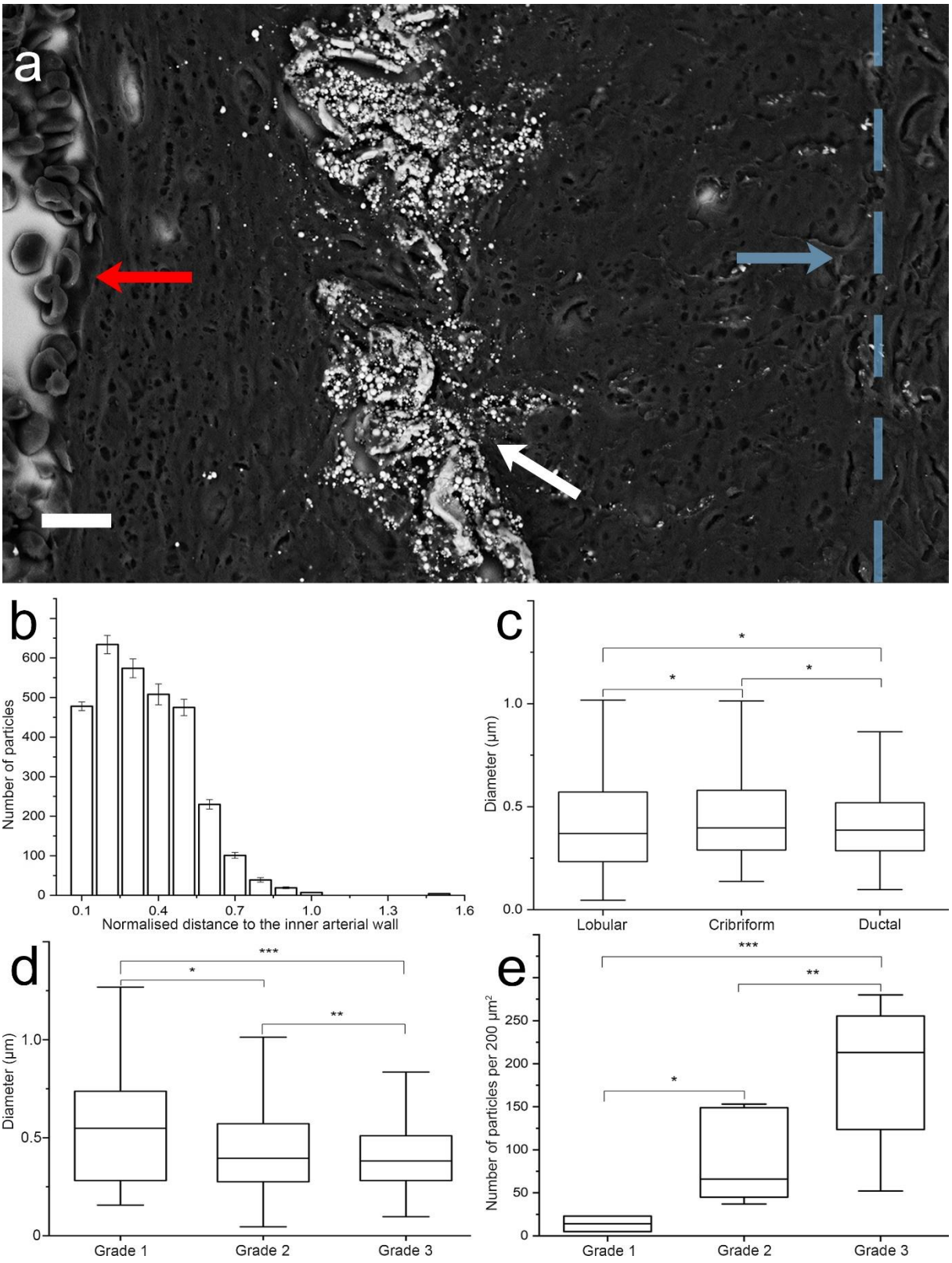


**Figure 2. Dimensions and occurrence of whitlockite nanoparticles. a** Representative backscattered electron micrograph of arterial wall tissue with the lumen indicated by a red arrow showing calcified accumulation of particles within the arterial wall. The end of the arterial wall is indicated by the blue line and arrow. **b** Position of 3000 nanoparticles as distributed within the arterial wall. Error bars indicate standard deviation. **c** Particle diameter for different types of malignancy (lobular, cribriform and ductal (n = 300)). (mean ± SD). One-way ANOVA

with Dunnett's T3 multiple comparisons post-hoc test. (*p > 0.9999). **d** Particle diameter in samples with different grades of malignancy (grade 1, grade 2 and grade 3 (n = 30, n = 600, n = 600)) (mean ± SD). One-way ANOVA with Dunnett's T3 multiple comparisons post-hoc test. (*p = 0.1436, **p > 0.9999, ***p =0.0294). **e** Spatial density distribution of particles in relation to different grades of malignancy (grade 1, grade 2 and grade 3 (n = 2, n = 5, n = 5)) (mean ± SD). One-way ANOVA with Dunnett's T3 multiple comparisons post-hoc test. (*p = 0.0298, **p = 0.2710, ***p =0.0898).

A correlation was also found between the number of particles and the grade of cancer; the number of particles in grade 1 tumours are significantly lower than in grade 2 and grade 3 tumours (Fig. 2e). Therefore, the number of spherical particles with tumor grade, indicates that they may accumulate over time as the cancer progresses.

In summary, the presence of spherical whitlockite particles provides a new biopsy marker for malignant breast cancer, and their size and concentration can be related to tumour grade. Also, interestingly, particles with of the same size, composition, morphology and crystallinity have previously been observed in the cardiovascular system[17,22] and on the Bruch's membrane of the human eye[23]. However, their impact on tumour tissue remains to be elucidated.

**Acknowledgements**

The authors would like to thank Shweta Agarwal for her assistance with FIB and TEM analyses. We also thank Charalambos Kallepitis for early discussions and suggestions for particle size measurement. We gratefully acknowledge support from the Rosetrees Trust (A1153) and the Strategic Focal Area Personalized Health and Related Technologies (SFA-PHRT) program of the ETH domain (I.K.H). We would like to thank Breast Cancer Now Tissue Bank for providing the samples and Uma Ekbote from Breast Cancer Now Tissue Bank for all her help. We would also like to thank Francesca Launchbury and Angela Richard-Londt, from the UCL IQPath Institute of Neurology, for their help with histological analyses and Alba Rodríguez Meira for her help with sample preparation.

## References


1 Naseem, M. *et al.* Mammographic microcalcifications and breast cancer tumorigenesis: a radiologic-pathologic analysis. *BMC cancer* **15,** 307(2015).

2 Kim, K. I. *et al.* Changing patterns of microcalcification on screening mammography for prediction of breast cancer. *Breast Cancer Tokyo* **23,** 471-478 (2016).

3 Wilkinson, L., Thomas, V. & Sharma, N. Microcalcification on mammography: approaches to interpretation and biopsy. *Br. J. Radiol.* **90,** 20160594 (2017).

4 Rominger, M. B., Steinmetz, C., Westerman, R., Ramaswamy, A. & Albert, U. S. Microcalcification-Associated Breast Cancer: Presentation, Successful First Excision, Long-Term Recurrence and Survival Rate. *Breast Care (Basel)* **10,** 380-385 (2015).

5 Scott, R., Kendall, C., Stone, N. & Rogers, K. Elemental vs. phase composition of breast calcifications. *Sci. Rep.* **7,** 136 (2017).

6 Kunitake, J. *et al.* Correlative imaging reveals physiochemical heterogeneity of microcalcifications in human breast carcinomas. *J. Struct. Biol.* **202**, 25-34, doi:10.1016/j.jsb.2017.12.002 (2018).

7 Haka Abigail S., S.-P. K. E., Fitzmaurice Maryann, Crowe Joseph, Dasari Ramachandra R., Feld Michael S. Identifying Microcalcifications in Benign and Malignant Breast Lesions by Probing Differences in Their Chemical Composition Using Raman Spectroscopy. *Cancer Res.* **61,** 5375-5380 (2002).

8 Ben Lakhdar, A. *et al.* Underlining the complexity of the structural and chemical characteristics of ectopic calcifications in breast tissues through FE-SEM and μFTIR spectroscopy. *C. R. Chimie* **19,** 1610-1624 (2016).

9 Morgan, M. P., Cooke, M. M. & McCarthy, G. M. Microcalcifications Associated with Breast Cancer: An Epiphenomenon or Biologically Significant Feature of Selected Tumors? *J. Mammary Gland Biol. Neoplasia* **10,** 181-187 (2005).

10 Ferranti C., e. a. Relationships between age, mammographic features and pathological tumour characteristics I non-palpable breast cancer. *Br. J. Radiol.* **73,** 698-705 (2000).

11 O'Grady, S. & Morgan, M. P. Microcalcifications in breast cancer: From pathophysiology to diagnosis and prognosis. *Biochim. Biophys. Acta Rev. Cancer* **1869,** 310-320 (2018).

12 Scott, R., Stone, N., Kendall, C., Geraki, K. & Rogers, K. Relationships between pathology and crystal structure in breast calcifications: an in situ X-ray diffraction study in histological sections. *npj Breast Cancer* **2,** 16029 (2016).

13 Cox, R. F. *et al.* Microcalcifications in breast cancer: novel insights into the molecular mechanism and functional consequence of mammary mineralisation. *Bri. J. Cancer* **106,** 525-537 (2012).

14 Choi, S., Coonrod, S., Estroff, L. & Fischbach, C. Chemical and physical properties of carbonated hydroxyapatite affect breast cancer cell behavior. *Acta Biomater.* **24,** 333-342 (2015).

15 Baker, R., Rogers, K. D., Shepherd, N. & Stone, N. New relationships between breast microcalcifications and cancer. *Bri. J. Cancer* **103,** 1034-1039 (2010).

16 Radenkovic, S. *et al.* HER2-positive breast cancer patients: correlation between mammographic and pathological findings. *Radiat. Prot. Dosimetry* **162,** 125-128 (2014).

17 Bertazzo, S. *et al.* Nano-analytical electron microscopy reveals fundamental insights into human cardiovascular tissue calcification. *Nat. Mater.* **12,** 576-583 (2013).

18 Scimeca, M. *et al.* Microcalcifications in breast cancer: an active phenomenon mediated by epithelial cells with mesenchymal characteristics. *BMC cancer* **14,** 286 (2014).

19 Frappart, L. *et al.* Structure and composition of microcalcifications in benign and malignant lesions of the breast: Study by light microscopy, transmission and scanning

electron microscopy, microprobe analysis, and X-ray diffraction. *Hum. Pathol.* **15,** 880-889 (1984).

20 Kunitake, J. A. M. R. *et al.* Correlative imaging reveals physiochemical heterogeneity of microcalcifications in human breast carcinomas. *J. Struct. Biol.* **202,** 25-34 (2018).

21 Hossler, F. E. *Ultrastructure Atlas of Human Tissues*. 303-358 (Hoboken, Jersey, 2014).

22 Bertazzo, S., Steele, J. A. M., Chester, A. H., Yacoub, M. H. & Stevens, M. M. Cardiovascular calcification violet pearl. *Lancet* (2014).

23 Tan, A. C. *et al.* Calcified nodules in retinal drusen are associated with disease progression in age-related macular degeneration. *Sci. Transl. Med.* **10,** eaat4544 (2018).

## Materials and Methods

*Sample preparation:* 81 samples were analysed (Supplementary Table S1) in total. The samples were obtained from the Department of Surgery and Cancer at the Imperial Centre for Translational and Experimental Medicine (UK), Breast Cancer Now Tissue Bank (UK) and the Cantonal Hospital of St. Gallen (Switzerland). For the collection of these samples, informed signed consent was obtained from either the patient or from next of kin and the samples were processed, analysed and disposed according to the ethical approval obtained. Histological specimens were prepared as per standard clinical protocols; 3-5µm thick, formalin-fixed, paraffin-embedded, and mounted on glass slides. The dewaxing of samples, required for imaging studies, was done using pure xylene solutions, at 5-minute intervals. Samples were coated with silver conductive paint and with carbon, using a Quorum K975X coater prior to imaging.

*Scanning Electron Microscopy:* Following sample preparation, a Hitachi S-3499N and a Carl Zeiss Crossbeam were used imaging with secondary electron (SE) and backscattering electron (BSE) modes. Using these two imaging modalities, density-dependent images (DDC-SEM) were also acquired. Energy-dispersive X-ray spectroscopy (EDX) analysis was carried out using Oxford Instruments EDX detectors, integrated into both microscopes. For this analysis, accelerating voltages of 5kV and 10kV and a working distance of 10mm were used.

*Histology:* Histopathological slides of breast cancer biopsies were produced using standard preparation procedures. The tissue was formalin-fixed and paraffin-embedded, and then cut into sections of 3-5µm in thickness, using a microtome. Haematoxylin and Eosin (H&E) staining was carried out on the slides, which were scanned using a Leica SCN400 scanner.

*Focused Ion Beam:* A FEI Helios NanoLab 600 DualBeam Focused Ion Beam System was used. A micro region of each sample was coated with a Platinum layer at 30kV and 93pA. Following this procedure, currents between 93pA and 2.8nA were used for section lift out and thinning to 100nm.

*Transmission Electron Microscopy:* FIB prepared sections were imaged using a JEOL JEM 2100Plus Transmission Electron Microscope at 200kV and 120kV.

*Size and distribution of calcific particles:* Dimension and count measurements were done manually using Image J. Data is expressed as mean ± standard deviation (SD) and was analysed using a One-way ANOVA with Dunnett's T3 multiple comparisons post-hoc test. The statistical significance was evaluated using a p value of 0.05. For all box plots the whiskers indicate the outlier values outside 1.5 times the interquartile ranges, and the box lines indicate the upper quartile, median, and lower quartile.